

Comparison of two PV array models for the simulation of PV systems using five different algorithms for the parameters identification



Sofiane Kichou^{a,*}, Santiago Silvestre^a, Letizia Guglielminotti^a, Llanos Mora-López^b, Emilio Muñoz-Cerón^c

^a MNT Group, Electronic Engineering Department, UPC-BarcelonaTech, Barcelona, C/ Jordi Girona 1-3, Mòdul C4 Campus Nord UPC, 08034 Barcelona, Spain

^b Dpto. Lenguajes y Ciencias de la Computación, Universidad de Málaga, Campus de Teatinos, sn, Málaga 29071, Spain

^c IDEA Research Group, University of Jaén, Campus de Las Lagunillas, 23071 Jaén, Spain

ARTICLE INFO

Article history:

Received 19 April 2016

Received in revised form

30 June 2016

Accepted 3 July 2016

Keywords:

PV modeling

Simulation

Parameter extraction

Metaheuristic algorithms

ABSTRACT

Simulation is of primal importance in the prediction of the produced power and automatic fault detection in PV grid-connected systems (PVGCS). The accuracy of simulation results depends on the models used for main components of the PV system, especially for the PV module. The present paper compares two PV array models, the five-parameter model (5PM) and the Sandia Array Performance Model (SAPM). Five different algorithms are used for estimating the unknown parameters of both PV models in order to see how they affect the accuracy of simulations in reproducing the outdoor behavior of three PVGCS. The arrays of the PVGCS are of three different PV module technologies: Crystalline silicon (c-Si), amorphous silicon (a-Si:H) and micromorph silicon (a-Si:H/ μ c-Si:H).

The accuracy of PV module models based on the five algorithms is evaluated by means of the Route Mean Square Error (RMSE) and the Normalized Mean Absolute Error (NMAE), calculated for different weather conditions (clear sky, semi-cloudy and cloudy days). For both models considered in this study, the best accuracy is obtained from simulations using the estimated values of unknown parameters delivered by the ABC algorithm. Where, the maximum error values of RMSE and NMAE stay below 6.61% and 2.66% respectively.

© 2016 Elsevier Ltd. All rights reserved.

1. Introduction

The photovoltaic (PV) market has grown rapidly in recent years worldwide, especially in developed countries, where this growth has been exponential. One of the main reasons for the high growth of the PV industry is the reduction of the cost of PV generation as well as the improvement of the quality and performance of the electronics associated with these generation systems. The monitoring and regular performance supervision on the functioning of grid-connected PV systems is basic to ensure an optimal energy harvesting and reliable power production at competitive costs. Detecting faults in PV systems can minimize generation losses by reducing the time in which the system is working below its point of maximum power generation. In this context, the development of

accurate automatic fault detection procedures is crucial [1–3]. Main faults in PV systems are caused by short circuits or open circuits in PV modules, inverter disconnections and the presence of shadows on the PV array plane [4–6].

On the other hand, the integration of grid-connected PV systems also requires the capability of managing the uncertainty related to the fluctuating energy output inherent to these generation plants. For this purpose, it is very important to develop accurate forecasting models in order to achieve an easy integration of PV generation plants into traditional power distribution systems [7,8].

Simulation plays a crucial role in both outdoor behavior forecasting and automatic fault detection of grid-connected PV systems. The precision of simulation results depends on the models used for the main components of the PV system, especially the PV module models [9,10]. Moreover, the accuracy of the PV module models is strongly affected by the way of extracting their unknown parameters. Several research works discussed the topic of PV model parameters estimation, by applying different methods based on analytical [11], numerical [12,13] and bio-inspired optimization solution [14–20].

* Corresponding author.

E-mail addresses: kichousofiane@gmail.com (S. Kichou), Santiago.silvestre@upc.edu (S. Silvestre), letizia.guglielminotti@gmail.com (L. Guglielminotti), llanos@lcc.uma.es (L. Mora-López), emunoz@ujaen.es (E. Muñoz-Cerón).

Previous works investigated the accuracy of PV module models focusing on the I-V curve of the PV module [21–24] or on the I-V characteristic of a PV array [25]. The objective of this study is to compare two PV array models to analyze the simulation of grid-connected PV systems in real conditions of work. The accuracy of the simulations in reproducing the actual behavior of the PV system is evaluated by means of the results obtained from different parameter extraction techniques based on five algorithms: Levenberg–Marquardt algorithm (LMA), genetic algorithm (GA), particle swarm optimization (PSO), differential evolution (DE) and artificial bee colony (ABC) algorithm.

The two PV array models included in this study are the five-parameter model (5PM) [26,27] and the Sandia Array Performance Model (SAPM) developed by Ref. [28]. Three real grid-connected PV systems are included in the study to validate the accuracy of the models. Each one of the PV systems is formed by PV modules of different technologies: Crystalline silicon (c-Si), amorphous silicon (a-Si:H) and micromorph silicon (a-Si:H/ μ c-Si:H) in order to outline differences in the prediction due to solar cell type.

The remainder of the paper is organized as follows: In Section 2, the PV systems included in the study are described. The PV array models and the parameters extraction techniques used in this study are summarized in Sections 3 and 4 respectively. Results obtained are shown in Section 5. Finally, conclusions are detailed in Section 6.

2. Description of the PV systems

Three grid connected PV systems formed by PV modules of different technologies were used in this study.

The first PV system is located in San Sebastián (Spain). The PV array is formed by 30 c-Si PV modules with a peak power of 4.8 kWp connected to a single phase inverter.

The other two PV systems are sited in Jaén (Spain). Each PV array is connected to single phase inverter with AC nominal powers of 1.2 kW. One of the PV arrays is formed of 15 a-Si:H PV modules, rated 60-W peak, and the second PV array consists of 8 micromorph PV modules, rated 110-Wp each. Main characteristics of the PV systems and PV modules forming the arrays are given in Table 1 and Table 2 respectively.

The following parameters were monitored in the three PV arrays: Current, voltage, power (DC and AC), cosine (φ), frequency, irradiance and module temperature with a sampling rate of 5 min.

In the PV system located in San Sebastián, the irradiance was measured by using a calibrated solar cell installed in the plane of the modules. The module temperature was measured using a Pt100 sensor fitted to the back of the module, in the middle of a cell. The

internal data acquisition card of the inverter recorded both parameters.

The monitoring system included in the PV arrays located in Jaén consists of three SMA Sunny SensorBox devices, installed in the same plane as the PV generators, capable to measure solar radiation, module and ambient temperatures together with wind speed. Two Pt100 RTD were pasted to the rear surface of the modules under test to measure the cell temperature in each PV array. An anemometer and a temperature probe were also available. All sensors were supplied by SMA and connected to three Sunny SensorBox devices. An additional irradiance sensor, aKipp & Zonen CMP11 pyranometer, was also installed and connected to one of the latter devices. The three of them were serially connected to the inverters via a RS-485 bus and then to a Sunny Webbox, from which environmental and operation could be retrieved.

3. PV array models

As it has been previously mentioned, the two PV array models included in this study are the 5PM [26,27,29] and the SAPM developed by Ref. [28].

The 5PM, also called one diode model, is one of the most used in simulation of PV modules and arrays. Moreover, root mean square errors (RMSE) of 4.26% [3], 4.39% [30] and 5.12% [31] were reported in the estimation of the energy produced by grid-connected PV systems in simulations of dynamic behavior of c-Si PV generators by using this model. On the other hand, simulations of a-Si PV arrays by using the SAPM model have obtained errors below 4.1% on sunny days [32]. In our approach, the model parameters are calculated by means of parameter extraction methods having as main input data daily actual profiles of module temperature, irradiance on the PV array plane and output voltage and current of the PV array.

3.1. Five-parameter model

The 5PM of a solar cell includes a parallel combination of a photogenerated controlled current source I_{ph} , a diode, described by the well-known single-exponential Shockley equation [33], a shunt resistance R_{sh} and a series resistance R_s modeling the power losses.

The I-V characteristic of a solar cell is given by an implicit and nonlinear equation as follows:

$$I = I_{ph} - I_o \left(e^{\left(\frac{V + R_s I}{n V_t} \right)} - 1 \right) - \left(\frac{V + R_s I}{R_{sh}} \right) \quad (1)$$

where I_o and n are the reverse saturation current and ideality factor of the diode respectively and V_t is the thermal voltage.

Table 1
PV systems description.

Main Parameters	PV system 1	PV system 2	PV system 3
PV Module	c-Si	a-Si:H/ μ c-Si:H	a-Si:H
Location	San Sebastián (Spain) Latitude: 43° 17' 9.8" N Longitude: 1° 59' 55.4" W Altitude: 41 m.	Jaén (Spain) Latitude: 37° 47' 14.35" N Longitude: 3° 46' 39.73" W Altitude: 511 m	
Nominal power	4.8 kWp	880 Wp	900 Wp
Modules per inverter	30	8	15
Modules in series (N_{sg})	15	4	3
Strings in parallel (N_{pg})	2	2	5
Tilt - Orientation	20° – 9° East	30° – 0° South	35° – 0° South
Inverter	Ingecon SUN 5 Single-phase inverter 5 kW	Sunny Boy SB1200 Single-phase inverter 1.2 kW	

Table 2
Main parameters of PV modules.

PV module Parameters	PV system 1	PV system 2	PV system 3
Isc (A)	9.46	2.5	1.19
Voc (V)	22.2	71	92
Current at Maximum Power Point: Impp (A)	8.65	2.04	0.9
Voltage at Maximum Power Point: Vmpp (V)	18.5	54	67
Temperature Coefficient of Voc β_{voc} (V/°C)	-0.084	-0.248	-0.280
Temperature Coefficient of Isc α_{isc} (A/°C)	4.60×10^{-3}	1.40×10^{-3}	0.89×10^{-3}

Eq. (1) can also be written as follows,

$$I = I_{ph} - I_d - I_{sh} \quad (2)$$

where I_d and I_{sh} are the currents across the diode and shunt resistance respectively.

The photogenerated current can be evaluated for any arbitrary value of irradiance, G , and cell temperature, T_c , by using the following equation:

$$I_{ph} = \frac{G}{G^*} I_{sc} + k_i (T_c - T_c^*) \quad (3)$$

where G^* and T_c^* are respectively the irradiance and cell temperature at standard test conditions (STC): 1000 W/m² (AM1.5) and 25 °C, k_i (A/°) is the temperature coefficient of the current and I_{sc} (A) is the solar cell short circuit current at STC.

Some PV modules are formed by parallel strings of solar cells connected in series. However, most PV modules include one single string of solar cells. Therefore, the model of the solar cell can be scaled up to the model of the PV module using the following Eqs. (4)–(8):

$$I_M = N_p I \quad (4)$$

$$I_{scM} = N_p I_{sc} \quad (5)$$

$$V_M = N_s V \quad (6)$$

$$V_{ocM} = N_s V_{oc} \quad (7)$$

$$R_{sM} = \frac{N_s}{N_p} R_s \quad (8)$$

Where subscript M stands for ‘Module’, N_s is the number of solar cells connected in series and N_p is the number of parallel branches of solar cells forming the module.

Then, the output current of the PV module, I_M , is obtained rewriting Eq. (2) as follows:

$$I_M = N_p (I_{ph} - I_{dM} - I_{shM}) \quad (9)$$

The diode current, I_{dM} , included in Eq. (9) is given by:

$$I_{dM} = I_{oM} \left[e^{\left(\frac{V_M + I_M R_{sM}}{n N_s V_t} \right)} - 1 \right] \quad (10)$$

where V_M (V) and I_M (A), are the output voltage and current of the PV module respectively.

The saturation current of the diode I_{oM} (A) depends strongly on temperature and it is given by:

$$I_{oM} = \frac{I_{scM} e^{\left(\frac{E_{go} - E_g}{V_{to} - V_t} \right)}}{N_p \left(e^{\left(\frac{V_{ocM}}{n N_s V_{to}} \right)} - 1 \right)} \left(\frac{T_c}{T_c^*} \right)^3 \quad (11)$$

where I_{scM} and V_{ocM} are the short-circuit current and the open-circuit voltage of the PV module respectively, V_{to} is the thermal voltage at STC, E_g the energy bandgap of the semiconductor and E_{go} is the energy bandgap at $T = 0$ K.

The value of the energy bandgap of the semiconductor at any cell temperature T_c is given by:

$$E_g = E_{go} - \frac{\alpha_{gap} T_c^2}{\beta_{gap} + T_c} \quad (12)$$

where α_{gap} and β_{gap} are fitting parameters characteristic of the semiconductor.

Finally, the current I_{shM} , also included in Eq. (9) is given by the following equation:

$$I_{shM} = \frac{V_M + I_M R_{sM}}{N_p R_{shM}} \quad (13)$$

The same procedure can be applied to scale up the model of the PV module to the model of a PV array by taking into account the number of PV modules connected in series by string, N_{sg} , and the number of parallel strings in the PV array, N_{pg} [27].

3.2. SAPM model

The SAPM model is an empirical model defined by the following equations [28]. The PV array power at the maximum power point (MPP), P_{mp} (W), is evaluated as follows:

$$P_{mpg} = I_{mpg} \times V_{mpg} \quad (14)$$

where, I_{mpg} (A) and V_{mpg} (V) are the coordinates of the MPP of the PV array.

The model uses the normalized irradiance, E_e , defined as follows,

$$E_e = \frac{G}{G^*} \quad (15)$$

Then, the current and voltage of the MPP of the PV array can be calculated by using the following equations:

$$I_{mpg} = N_{pg} \left[I_{mpo} \left(C_0 E_e + C_1 E_e^2 \right) \left(1 + \alpha_{Imp} (T_c - T_c^*) \right) \right] \quad (16)$$

$$Vmpg = N_{sg} \left[Vmpo + C_2 N_s \delta(T_c) \ln(Ee) + C_3 N_s (\delta(T_c) \ln(Ee))^2 + \beta_{Vmp} Ee (T_c - T_c^*) \right] \quad (17)$$

$$\delta(T_c) = nk(T_c + 273.15)/q \quad (18)$$

where, I_{mpo} (A) and V_{mpo} (V) are the PV module current and voltage of the MPP at STC, C_0 and C_1 are empirically determined coefficients (dimensionless) which relate I_{mp} to the effective irradiance, $C_0 + C_1 = 1$, α_{Imp} ($^{\circ}C^{-1}$) is the normalized temperature coefficient for I_{mp} , C_2 (dimensionless) and C_3 (V^{-1}) are empirical coefficients which relate V_{mp} to the effective irradiance, $\delta(T_c)$ is the thermal voltage per cell at temperature T_c , q is the elementary charge, 1.60218×10^{-19} (coulomb), k is the Boltzmann's constant, 1.38066×10^{-23} (J/K) and β_{Vmp} ($V/^{\circ}C$) is the temperature coefficient for module V_{mp} at STC.

The models contain several coefficients and parameters that must be calculated because are not routinely provided by the PV module's manufacturer. For this purpose, we used the parameter extraction techniques described in the following section.

4. Parameter extraction techniques

The parameter extraction techniques employed in this study are based on five optimization algorithms that evaluate the model parameters of the two PV array models in real conditions of work, using as inputs daily profiles of solar irradiance and cell temperature together with monitored DC output current and voltage.

For the five-parameter model of the PV module, the model parameters: I_{ph} , I_0 , n , R_s , and R_{sh} are evaluated by using Eqs. (3)–(13) and actual daily profiles of monitored current and voltage at the DC output of the three PV arrays included in the study, together with actual daily profiles of G and T_c at the specific locations detailed in Section 2.

Regarding the SAPM, the same idea is considered for the estimation of the empirical coefficients of the model parameters: C_0 , C_1 , C_2 , C_3 , n , α_{Imp} and β_{Vmp} using Eqs. (15)–(18).

The objective function for optimization using metaheuristic algorithms is defined as the RMSE of the error of all data points given by Eq. (19) [19,34], where the N represent the number of measured data, V_i and I_i represent the measured voltage and current of the data point i .

$$S(\theta) = \sqrt{\frac{1}{N} \sum_{i=1}^N [I_i - I(V_i, \theta)]^2} \quad (19)$$

where $\theta = f(I_{ph}, I_0, n, R_s, R_{sh})$ for the five parameter model and $\theta = f(C_0, C_1, C_2, C_3, n, \alpha_{Imp}, \beta_{Vmp})$ for the SAPM.

The parameter extraction algorithms implemented in MATLAB/Simulink environment are executed until function $S(\theta)$, given by Eq. (19), is minimized. Figs. 1 and 2 show the Simulink block diagram of the 5PM and SAPM used in the parameter extraction procedures. Thus, the result of the parameter extraction algorithms is a set of PV module parameters for the 5PM and a set of empirical parameters for the SAPM that allow the best approach to the real daily evolution of DC output current and voltage of the PV arrays.

Two parameter extraction methods are used in this study. The first method is a numerical solution based on Levenberg–Marquardt algorithm (LMA) detailed in a previous work [12]. The second method is based on different metaheuristic algorithms (GA, DE, PSO and ABC) which are described below.

4.1. Genetic algorithm

The Genetic Algorithm (GA) developed by John Holland in the 1970s is a technique for solving constrained and unconstrained optimization problems inspired from the biological evolution.

The optimization function is encoded as arrays of binary character strings representing the chromosomes. The fitness of chromosomes in the population is evaluated by the objective function for each iteration. Fitter chromosomes are stochastically selected in terms of the elitist strategy, which ensures the progeny chromosomes inherit the best possible combination of the genes of their parents. Some of the chromosomes in the population are modified via genetic operators like crossover and mutation, forming new chromosomes for the next generation. The reason why GA applies crossover and mutation may lie in their capability of avoiding local optima in the searching process. Several researches applied GA to extract the parameters of a PV model from measured I–V curves [17,35].

In this paper, the genetic algorithm available in the Global Optimization toolbox of MATLAB has been used for minimizing the objective function Eq. (19) [17].

4.2. Differential evolution

Differential evolution (DE) was proposed by Rainer Storn and Kenneth Price in 1997 [36]. Similar to other evolutionary algorithms, DE is a population based, derivative-free function optimizer. An advantage of DE over GA is that DE treats possible solutions as real-number strings, and thus encoding and decoding are not required.

The target vector $x = [x_1, x_2, \dots, x_i]$ where $i = 1, 2, \dots, NP$ represents a population of NP random candidate solutions. The vector of the i th particle, x_i indicates a series of parameters to be extracted, e.g. $x_i = [I_{ph}, I_0, n, R_s, R_{sh}]$ for the one-diode model and $x_i = [C_0, C_1, C_2, C_3, n, \alpha_{Imp}, \beta_{Vmp}]$. For a D -dimension optimization problem, a random candidate solution is given by:

$$x_j^{low} \leq x_{ij} \leq x_j^{up} \quad (20)$$

where x_j^{low} and x_j^{up} are the lower and the upper limits of the j th vector component respectively, $i = 1, 2, \dots, NP$ and $j = 1, 2, \dots, D$.

After the initialization DE enters a loop of evolutionary operations: mutation, crossover and selection considering the maximum number of generations t_{max} , where $t = 1, 2, \dots, t_{max}$.

In the mutation step, for each x_i at generation t , three vectors x_{r0} , x_{r1} and x_{r2} are chosen randomly from the set $\{1, 2, \dots, NP\} \setminus \{i\}$ to generate a donor vector by:

$$v_i^{t+1} = x_{r0}^t + F(x_{r1}^t - x_{r2}^t) \quad (21)$$

where F is a differential weight, known as scaling parameter, usually ranges in the interval $[0, 1]$.

The crossover operation is used to decide whether to exchange with donor vector. By generating a random integer index $J_r \in [1, D]$ and a randomly distributed number $k_i \in [0, 1]$, the j th dimension of v_i , namely u_{ij} , is updated according to:

$$u_{ij}^{t+1} = \begin{cases} v_{ij}^{t+1}, & k_i \leq CR \text{ or } i = J_r \\ x_{ij}^t, & k_i > CR \text{ and } i \neq J_r \end{cases} \quad (22)$$

where CR is a crossover probability in the interval $[0, 1]$. The crossover scheme formulated by Eq. (22) used in the present work is called binomial strategy.

The selection operation, selects the best one from the parent

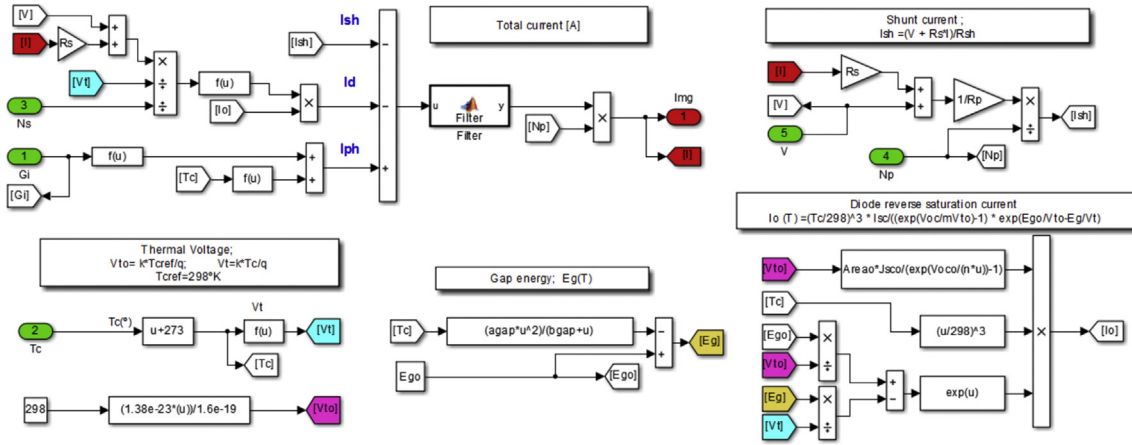


Fig. 1. Simulink block diagram for the 5PM.

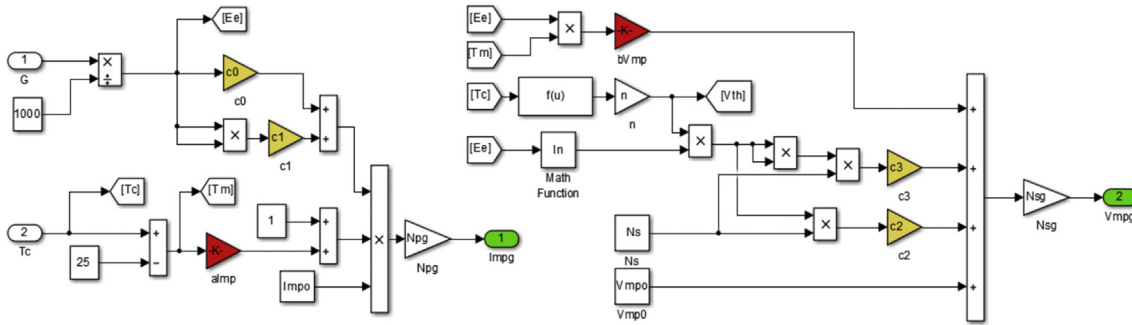


Fig. 2. Simulink block diagram for the SAPM.

vector x_i^t , and the trial vector u_i^{t+1} solution with the minimum objective value, using the following expression:

$$x_i^{t+1} = \begin{cases} u_i^{t+1}, & f(u_i^{t+1}) \leq f(x_i^t) \\ x_i^t, & \text{otherwise} \end{cases} \quad (23)$$

where $f(x)$ is the fitness function to be minimized. Therefore, if a particular trial vector is found to result in lower fitness value, it will replace the existing target vector; otherwise, the target vector is retained.

4.3. Particle swarm optimization

Particle swarm optimization (PSO) is a population based stochastic optimization technique developed by Kennedy and Eberhart [16] and is inspired by the social behavior of bird flocking or fish schooling.

PSO search possible solution in a search space by adjusting the trajectories of particles. The best position encountered of the particle i is designed by $pbest_i$. In a swarm of particles, there are N local best positions, and the best solution is denoted by $gbest$.

The velocities and positions of particles, as well as the algorithm parameters (inertia weight w and learning parameters α , β) are firstly initialized. In an iteration t , the fitness of particles is evaluated individually by the objective function. By attracted toward $pbest_i$ and $gbest$, the particle moves according to the following expression:

$$x_i^{t+1} = x_i^t + v_i^{t+1} \quad (24)$$

where v_i^{t+1} is the velocity, expressed as:

$$v_i^{t+1} = wv_i^t + \alpha\varepsilon_1(x_i^t - gbest^t) + \beta\varepsilon_2(x_i^t - pbest_i^t) \quad (25)$$

$\alpha = 1.5$, $\beta = 2$. The random vectors ε_1 and ε_2 are in the range $[0, 1]$. The w is the inertia weight, used to balance global and local search abilities, it is considered constant and set equal to 0.9.

Finally, lower and upper boundaries are set to ensure that particles are within the predetermined range. The PSO will continue to search for better solutions until it meets the stopping criterion.

4.4. Artificial bee colony algorithm

The artificial bee colony algorithm (ABC) is an optimization algorithm inspired by the natural foraging behavior of honey bees. It was successfully applied in the parameter extraction of solar cell models [19,34]. In the ABC, there are food sources representing the solutions of optimization problems and honey bees (classified into employed bees, onlooker bees and scout bees) representing the operations to the solutions. The employed bees investigate potential food sources and share information with onlooker bees. The food sources of higher quality will have higher possibility to be selected by onlooker bees. If the quality of the employed bees' food sources is relatively low, they will change to scout bees to randomly explore new potential food sources. Consequently, the exploitation is promoted by employed and onlooker bees while the exploration is performed by scout bees. The implementation of the ABC algorithm in MATLAB is carried out by following the same steps of given in the previous works [19,34,37].

5. Results

The results of simulation of grid-connected PV systems in real conditions of work were obtained under different weather conditions: clear sky, semi-cloudy, and cloudy weather. The two PV array models described above were used for forecasting the output power of the three different PV systems using the extracted parameters delivered by the five algorithms.

The adjustable parameters chosen for the GA, DE, PSO and ABC algorithms and the lower and upper boundaries selected for each parameter are summarized in Tables 3 and 4.

The optimization algorithms used in the parameter extraction techniques evaluate the model parameters of the PV module; I_{ph} , I_o , n , R_s , R_{sh} , in case of the 5PM, and C_0 , C_1 , C_2 , C_3 , n , α_{imp} , β_{vmp} , in case of SAPM.

In the case of using the extraction method based on LMA, an average number of 10 iterations are needed in order to find a set of solar cell model parameters for an input data set corresponding to one day of real operation of the PV array. On the other hand, for the extraction method relied on the metaheuristic algorithms (GA, PSO, DE and ABC) the average number of iterations is much higher, by around 500 iterations are needed.

Moreover, the parameter extraction methods were applied for each sample day separately, in order to get the optimal set of parameters of the two PV models that allows reproducing the real behavior of the PV systems with best accuracy. As the extracted parameters values obtained by the different algorithms are very close to each other, it is decided to show the mean value of each extracted parameter. The set of the extracted parameters are listed in Tables 5 and 6.

In order to present the best variety of results, and see the performance of the two models using real conditions of solar irradiance and cell temperature, it was chosen to display the DC output current evolution over the course of a clear sky day for PV system 1, a semi-cloudy day for PV system 2 and a cloudy day for PV system 3.

Figs. 3–8 show the measured DC output current of the three PV systems, compared with the simulation results obtained with the two PV array models using the extracted set of parameters estimated by the five optimization algorithms considered in this study.

As it can be seen in the figures, a good agreement is always found between the measured data and the SAPM simulation curves, while the curves obtained with the 5PM are less close to the real monitored curve. Moreover, it is found that a better agreement between real and simulated curve is always reached in clear sky days rather than in cloudy days. It is qualitatively noted that the worse the weather conditions, the more difficult is for the models to approximate real data as expected.

By comparing the optimization algorithms used for the estimation of the unknown parameters of the two PV array models, it can be clearly seen that the metaheuristic algorithms provide good results compared to the LMA in all weather conditions and for both PV models.

These considerations are confirmed by values of errors

Table 3 Selected parameters of each algorithm

Algorithm parameters	GA	PSO	DE	ABC
Population (colony) size, (NP)	100	100	100	100
Inertia weight, (w)	–	0,9	–	–
α and β	–	1.5 and 2	–	–
Crossover probability (CR)	–	–	0.4	–
Number of onlooker bees	–	–	–	50
Limit of scout bees	–	–	–	420
Maximum number of iteration	1000	1000	1000	1000

Table 4 Lower and upper boundaries selected for each PV module model parameter.

C_0	[0–2]	I_{ph} [A]	[0–10]
C_1	[–1–1]	I_o [A]	$[10^{-7}-10^{-11}]$
C_2	[–10–10]	n	[1–2]
C_3	[–10–100]	R_s [Ω]	[0–20]
α_{imp} [$^{\circ}C^{-1}$]	$[10^{-4}-10^{-2}]$	R_{sh} [Ω]	$[50-10^5]$
β_{vmp} [V/ $^{\circ}C$]	[–1–0]		

calculated for the two PV models given in Tables 7 and 8. The values quantify discrepancies between measured data (DC output current, voltage and power) versus simulated ones predicted by the two PV array models using the five algorithms (LMA, GA, PSO, DE and ABC). Two metrics were used: The Route Mean Square Error (RMSE) [32] and the Normalized Mean Absolute Error (NMAE) [10]. For the error calculation an irradiance filter was applied to the data set. Only the data corresponding to irradiance values above 200 W/m² were considered, since the inverters start working in these conditions. Below this irradiance value, the PV systems are in an open circuit configuration, and the resulting values are misleading.

The DC output power of the PV array is obtained as a product of current and voltage in both real and simulated results.

As a general trend, the errors obtained in the case of SAPM model were smaller than in the case of the 5PM for all PV systems and weather conditions regardless of the solar cell technology. Similarly, for each PV system the error decreases with improving weather conditions: The error for clear sky day was smaller than for semi-cloudy day, while for cloudy day the largest discrepancy was always found, as anticipated from the inspection of Figs. 3–8.

The maximum values of RMSE and NMAE obtained for the output power using the SAPM model were 6.02% and 2.40% respectively. These values were provided by simulations based on LMA of the PV system 1 with c-Si PV modules in a cloudy day. Nevertheless, for the PV systems 2 and 3 based on different PV module technologies, the RMSE and NMAE errors obtained for DC output power were below 4% and 1.86 %.

On the other hand, in the simulations based on the 5PM the maximum values of RMSE and NMAE obtained regarding the DC output power were increased up to 13.55% and 5.30% for PV system 1 based on LMA. However, for the PV systems 2 and 3, even based on the LMA, the obtained values of RMSE and NMAE were 6.99% and 3.29 %.

The accuracy of the PV module models in reproducing the behavior of the PV array under outdoor conditions of solar irradiance and cell temperature depends also on the used methods for parameters estimation. As it can be seen from Tables 7 and 8, the metaheuristic algorithms provide lower values of RMSE and NMAE than the numerical traditional method based on the LMA.

Considering the SAPM, the passage from using the LMA to GA as a main algorithm of the parameter extraction, reduces the maximum values of RMSE and NMAE of the DC output power to 5.84% and 2.35% taking into account all the PV systems and weather conditions. This passage from LMA to GA also affects the accuracy of the 5PM, where the maximum values of RMSE and NMAE of the DC output power were reduced to 11.23% and 4.12% respectively.

The best accuracy of simulations using the SAPM was obtained by using the ABC algorithm for the estimation of the unknown parameters. The greatest RMSE and NMAE values obtained regarding the DC power of the PV system 1 were 5.78% and 2.26%. Otherwise for PV system 2 the errors values don't exceed 3.13% and 1.61%, and for PV system 3 the best accuracy is achieved, whatever the weather condition, the RMSE and NMAE are below 1.43% and 1.02% respectively.

On the other hand, for the 5PM, the best forecasting of the DC

Table 5
Mean values of the main PV module parameters obtained from the parameter extraction algorithms for the 5PM.

PV system	Day	Weather conditions	R_s [Ω]	R_{sh} [Ω]	I_o [A]	I_{ph} [A]	n
1	09/12/2013	Clear sky	0.662	660.011	1.07×10^{-8}	8.7268	1.191
	18/12/2013	Semi cloudy	0.701	651.880	1.14×10^{-8}	8.7366	1.192
	20/12/2013	Cloudy	0.701	651.894	1.14×10^{-8}	8.7366	1.192
2	05/07/2012	Clear sky	5.771	25.96×10^3	2.32×10^{-7}	2.2055	1.223
	12/05/2012	Semi cloudy	7.321	20.34×10^3	4.90×10^{-7}	2.2462	1.290
	12/11/2012	Cloudy	8.010	21.31×10^3	1.20×10^{-7}	2.2462	1.289
3	07/08/2011	Clear sky	12.354	3.358×10^3	8.82×10^{-9}	1.0751	1.343
	12/05/2012	Semi cloudy	17.915	2.365×10^3	7.92×10^{-9}	1.0627	1.351
	12/11/2012	Cloudy	19.796	2.865×10^3	1.36×10^{-9}	1.0686	1.351

Table 6
Average values of main parameters obtained from the parameter extraction algorithms for the SAPM.

PV System	Day	Weather conditions	C_0	C_1	C_2	C_3	n	α_{Imp} [$^{\circ}C^{-1}$]	β_{Vmp} [V/ $^{\circ}C$]
1	09/12/2013	Clear sky	1.0438	-0.2000	2.0686	21.2425	1.1619	4.32×10^{-3}	-0.1067
	18/12/2013	Semi cloudy	0.9138	-0.0552	1.6104	10.9348	1.1613	4.32×10^{-3}	-0.1168
	20/12/2013	Cloudy	0.9762	-0.1468	2.0351	12.7702	1.162	4.32×10^{-3}	-0.0554
2	05/07/2012	Clear sky	0.8887	0.0662	2.575	31.7208	1.2177	5.8×10^{-4}	-0.2819
	12/05/2012	Semi cloudy	0.9237	0.0500	2.995	43.1182	1.2459	5.8×10^{-4}	-0.2692
	12/11/2012	Cloudy	0.9208	0.0608	2.4241	20.0134	1.2466	5.8×10^{-4}	-0.4632
3	07/08/2011	Clear sky	0.8229	0.0500	2.1346	18.999	1.3162	7.52×10^{-3}	-0.2467
	12/05/2012	Semi cloudy	0.7973	0.0400	2.7898	27.9781	1.3537	7.52×10^{-3}	-0.3299
	12/11/2012	Cloudy	1.0010	-0.1086	1.7077	7.8209	1.2941	7.52×10^{-3}	-0.4998

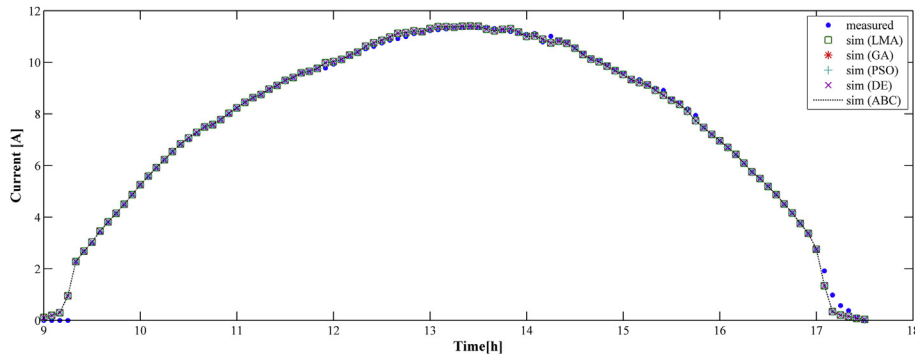


Fig. 3. Evolution of the DC-current of the PV system 1 using SAPM for clear sky day (December 09th, 2013).

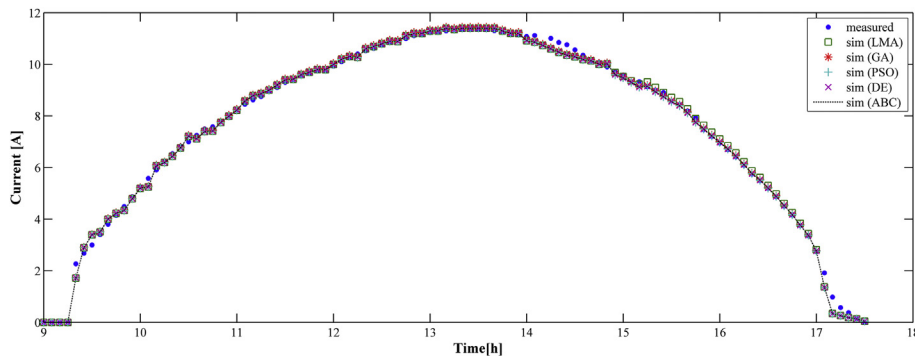


Fig. 4. Evolution of the DC-current of the PV system 1 using 5PM for clear sky day (December 09th, 2013).

output power of the PV systems is also obtained from simulations using the estimated parameters provided by the ABC algorithm. Considering the worst weather condition, the RMSE and NMAE values related to DC output power obtained for the PV system 1 are 6.6% and 2.67%. However, for the PV systems 2 and 3 the errors values remain below 3.65% and 2.07%.

Finally, regarding the DC output current, the highest values of RMSE obtained in clear sky and semi cloudy day, are below 2.91% in case of SAPM and 3.42% in case of 5PM. In order to make the obtained results more comprehensive, other machines learning used for modeling the DC output current of PV arrays were considered. Ameen et al. [13] reported RMSE of 5.67% in a work based on

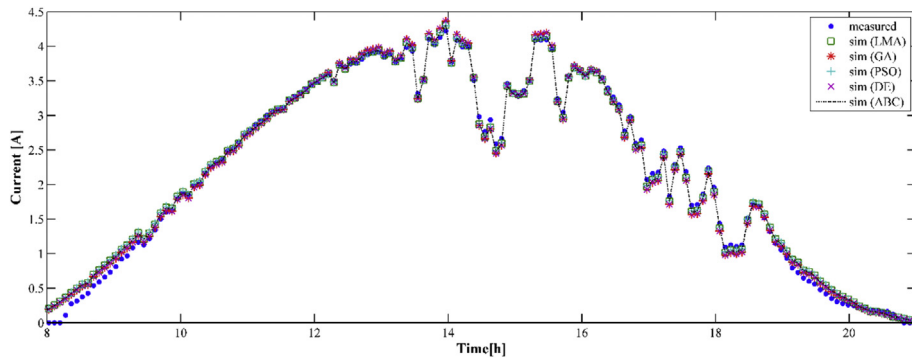


Fig. 5. Evolution of the DC-current of the PV system 2 using SAPM for semi-cloudy day (May 12th, 2012).

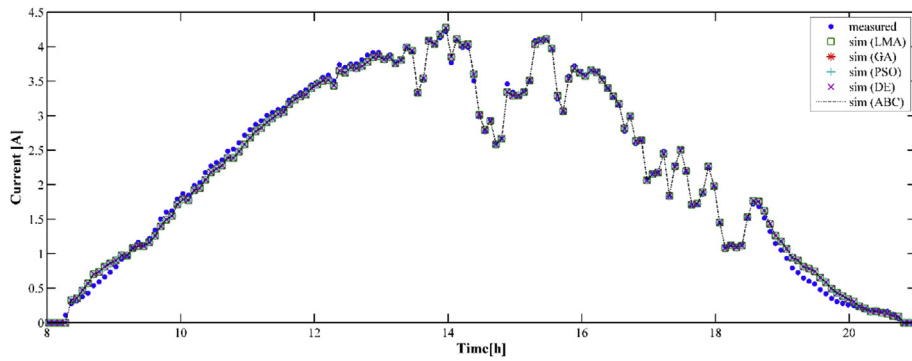


Fig. 6. Evolution of the DC-current of the PV system 2 using 5PM for semi-cloudy day (May 12th, 2012).

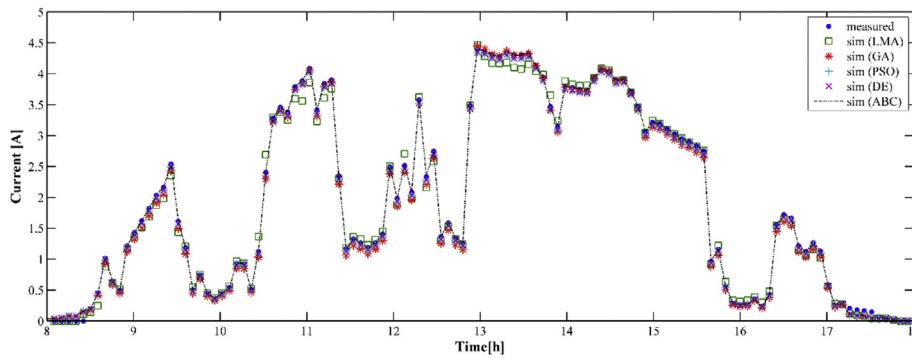


Fig. 7. Evolution of the DC-current of the PV system 3 using SAPM for cloudy day (November 12th, 2012).

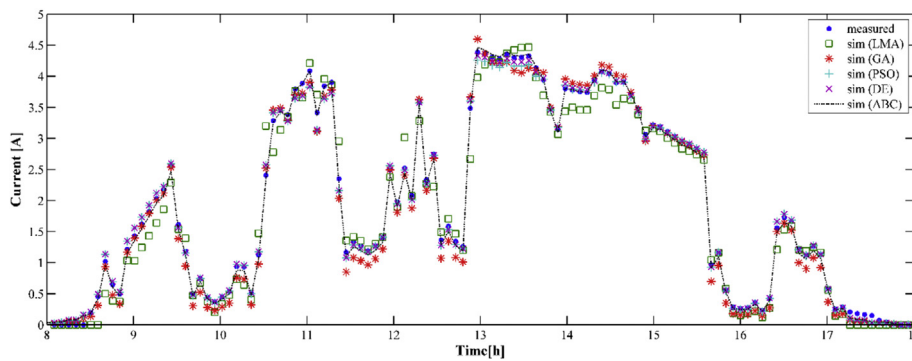


Fig. 8. Evolution of the DC-current of the PV system 3 using 5PM for cloudy day (November 12th, 2012).

Table 7
Calculated RMSE (%) and NMAE (%) for the SAPM.

PV system	Day	Weather	Error [%]	LMA			GA			PSO			DE			ABC		
				I	V	P	I	V	P	I	V	P	I	V	P	I	V	P
1	09/12/2013	Clear sky	RMSE	0.64	2.09	1.72	0.64	1.26	1.18	0.64	0.84	1.00	0.65	0.84	0.99	0.65	0.71	0.63
			NMAE	0.27	1.43	0.77	0.25	0.97	0.58	0.26	0.62	0.45	0.26	0.62	0.45	0.27	0.48	0.25
	18/12/2013	Semi cloudy	RMSE	2.91	4.09	2.87	2.51	2.98	2.68	2.50	2.98	2.63	2.50	2.90	2.59	2.50	2.89	2.59
			NMAE	1.29	2.11	1.12	0.86	1.83	0.97	0.83	1.84	0.94	0.83	1.70	0.89	0.83	1.69	0.91
	20/12/2013	Cloudy	RMSE	6.37	5.06	6.02	6.41	4.90	5.84	6.36	4.91	5.77	6.35	4.87	5.79	6.37	4.91	5.78
			NMAE	2.43	3.51	2.40	2.54	3.34	2.35	2.44	3.34	2.26	2.44	3.32	2.27	2.44	3.35	2.26
2	05/07/2012	Clear sky	RMSE	1.33	1.42	1.55	1.29	0.82	1.14	1.31	0.81	1.14	1.29	1.02	1.06	1.27	0.84	1.03
			NMAE	0.46	1.48	0.78	0.53	1.23	0.70	0.47	1.29	0.58	0.51	1.73	0.55	0.53	1.47	0.52
	12/05/2012	Semi cloudy	RMSE	1.54	1.13	1.55	1.52	0.98	1.53	1.52	1.11	1.41	1.75	1.49	1.36	1.53	1.11	1.32
			NMAE	0.62	1.67	0.88	0.59	1.50	0.88	0.59	1.90	0.87	0.75	2.68	0.85	0.61	1.89	0.83
	12/11/2012	Cloudy	RMSE	2.75	3.50	3.51	2.78	3.32	3.17	2.76	3.22	3.15	2.76	3.22	3.15	2.76	3.31	3.13
			NMAE	0.70	5.91	1.84	0.68	4.59	1.65	0.69	4.32	1.62	0.68	4.31	1.61	0.69	4.57	1.61
3	07/08/2011	Clear sky	RMSE	1.37	0.92	1.43	1.04	0.95	1.17	1.04	0.88	1.10	1.04	0.77	0.99	1.04	0.76	0.98
			NMAE	1.25	0.56	0.78	0.90	0.64	0.66	0.90	0.56	0.59	0.91	0.64	0.51	0.90	0.61	0.48
	12/05/2012	Semi cloudy	RMSE	1.91	0.89	2.20	1.23	0.81	1.10	1.24	0.90	0.93	1.24	0.82	1.07	1.23	0.89	0.91
			NMAE	1.70	0.81	1.07	1.05	0.68	0.49	1.08	0.82	0.43	1.07	0.68	0.48	1.07	0.81	0.41
	12/11/2012	Cloudy	RMSE	2.67	2.39	4.00	2.40	1.87	2.16	2.42	1.62	1.98	2.42	1.68	2.07	2.25	1.62	1.42
			NMAE	2.12	3.27	1.86	1.75	2.34	1.09	1.79	2.04	0.66	1.75	2.08	1.06	1.75	2.04	1.01

Table 8
Calculated RMSE (%) and NMAE (%) for the 5PM.

PV system	Day	Weather	Error [%]	LMA			GA			PSO			DE			ABC		
				I	V	P	I	V	P	I	V	P	I	V	P	I	V	P
1	09/12/2013	Clear sky	RMSE	1.78	1.39	2.29	1.76	1.39	2.23	1.75	1.39	2.22	1.75	1.38	2.21	1.75	1.38	2.21
			NMAE	0.89	0.98	1.05	0.88	0.98	1.05	0.88	0.98	1.05	0.87	0.97	1.04	0.87	0.96	1.04
	18/12/2013	Semi cloudy	RMSE	3.42	3.93	4.96	3.37	3.84	4.88	3.37	3.80	4.05	2.84	3.82	3.72	2.55	4.84	3.69
			NMAE	1.38	2.48	2.19	1.35	2.48	2.13	1.34	2.45	1.94	1.28	2.46	1.80	0.97	3.08	1.74
	20/12/2013	Cloudy	RMSE	10.34	4.92	13.55	9.34	5.80	11.23	7.73	4.87	6.96	6.41	6.29	7.79	5.60	4.91	6.60
			NMAE	4.37	3.63	5.30	4.30	3.51	4.12	3.63	3.32	2.91	3.17	4.76	2.99	2.14	3.62	2.67
2	05/07/2012	Clear sky	RMSE	1.35	2.07	2.43	1.34	2.07	2.42	1.34	2.06	2.41	1.34	2.06	2.40	1.34	1.38	2.09
			NMAE	0.48	3.03	1.59	0.48	3.02	1.59	0.48	3.03	1.59	0.47	3.01	1.57	0.47	2.47	1.45
	12/05/2012	Semi cloudy	RMSE	1.60	2.98	3.51	1.60	2.92	3.41	1.60	2.28	3.13	1.60	2.27	3.13	1.61	2.12	3.07
			NMAE	0.64	5.40	2.50	0.65	5.24	2.42	0.65	3.71	2.10	0.65	3.70	2.10	0.64	3.72	2.08
	12/11/2012	Cloudy	RMSE	4.13	3.24	5.01	3.16	3.25	4.86	2.44	2.98	3.98	3.70	3.24	4.60	3.50	3.14	3.64
			NMAE	1.53	5.83	3.87	1.15	5.83	3.17	0.87	5.09	2.54	1.27	5.83	2.72	1.16	5.29	2.06
3	07/08/2011	Clear sky	RMSE	1.91	2.44	3.32	1.90	2.43	3.31	1.91	2.16	1.57	1.83	1.92	2.12	0.85	2.31	1.28
			NMAE	1.61	1.77	1.71	1.60	1.75	1.73	1.61	1.59	1.69	1.09	0.89	1.01	0.79	1.88	0.67
	12/05/2012	Semi cloudy	RMSE	1.66	2.68	3.53	1.72	2.09	3.36	1.67	1.97	3.34	1.65	1.95	3.17	1.66	1.95	3.02
			NMAE	1.51	2.49	1.78	1.52	1.74	1.67	1.52	1.76	1.66	1.51	1.74	1.60	1.51	1.75	1.53
	12/11/2012	Cloudy	RMSE	5.36	5.10	6.99	3.44	5.10	4.84	2.53	2.36	2.63	2.12	2.52	1.89	2.09	2.53	1.78
			NMAE	4.25	3.22	3.29	2.76	3.21	2.44	1.89	2.18	1.42	1.60	2.24	0.91	1.51	2.26	0.80

artificial neural networks for forecasting the output current of a PV array. Ibrahim et al. [38] published a novel machine learning consisting in using random forests technique for modeling the output current of a PV array, the RMSE provided is of 2.74%.

6. Conclusions

Two PV array models have been compared in this work for simulation purposes: The 5PM and the SAPM. These models were applied to reproduce the behavior of three grid connected PV systems with different topologies and solar cell technologies. The models parameters were obtained from daily monitored profiles of G , T_c , and output DC current and voltage of the PV arrays using five different optimization algorithms (LMA, GA, PSO, DE and ABC).

The metaheuristic algorithms are more efficient than the traditional LMA algorithm in estimating the unknown parameters of both PV module models, essentially in bad weather conditions. The GA provides high values of RMSE compared to the other bio-inspired algorithms. The ABC algorithm is slightly more accurate than the DE and PSO algorithms.

The 5PM allowed simulating the dynamic behavior of the PV systems included in this study with an acceptable accuracy degree

for applications of supervision and forecasting of energy production. The RMSE obtained in the comparison of the daily evolution of main electrical parameters of the PV systems is below 8% in all cases except the case of using LMA and GA algorithms to simulate the c-Si PV module working in cloudy conditions. This effect can be explained taking into account that the values of series, R_s , and shunt, R_{sh} , resistances forming part of the model parameter set vary with the irradiance, whereas both parameters have been assumed constant in the performed simulations. An advantage of the 5PM lies in the physical meaning of the set of model parameters that provides relevant information about the PV array and allows an easy comparison between different PV modules.

On the other hand, the SAPM model is an empirical model including a set of model parameters in which some of them have little physical meaning. Nevertheless, the SAPM model showed a high accuracy degree in the simulation of the PV systems behavior independently of the solar cell technology. The RMSE values obtained for the DC output power of the PV arrays in the simulations stayed below 6.05% for the PV system 1 even in cloudy days. For the PV system 2 this error dropped below 3.52%. However, for the PV system 3 the RMSE values are below 4% even in cloudy days and case of using LMA. The SAPM model demonstrated best potential

for the simulation of PV systems in real operating conditions; this holds even when using thin film technologies of PV modules.

Acknowledgments

This work was partly supported by the Spanish Science and Innovation Ministry and the ERDF within the frame of the project 'Estimación de la energía generada por módulos fotovoltaicos de capa delgada: influencia del espectro' under expedient code ENE2008-05098/ALT.

References

- [1] C. Ventura, G.M. Tina, Development of models for on-line diagnostic and energy assessment analysis of PV power plants: the study case of 1 MW Sicilian PV plant, *Energy Procedia* 83 (2015) 248–257, <http://dx.doi.org/10.1016/j.egypro.2015.12.179>.
- [2] S. Silvestre, M.A. Da Silva, A. Chouder, D. Guasch, E. Karatepe, New procedure for fault detection in grid connected PV systems based on the evaluation of current and voltage indicators, *Energy Convers. Manag.* 86 (2014) 241–249, <http://dx.doi.org/10.1016/j.enconman.2014.05.008>.
- [3] a. Chouder, S. Silvestre, Automatic supervision and fault detection of PV systems based on power losses analysis, *Energy Convers. Manag.* 51 (2010) 1929–1937, <http://dx.doi.org/10.1016/j.enconman.2010.02.025>.
- [4] S. Silvestre, A. Chouder, E. Karatepe, Automatic fault detection in grid connected PV systems, *Sol. Energy* 94 (2013) 119–127, <http://dx.doi.org/10.1016/j.solener.2013.05.001>.
- [5] S. Silvestre, S. Kichou, A. Chouder, G. Nofuentes, E. Karatepe, Analysis of current and voltage indicators in grid connected PV (photovoltaic) systems working in faulty and partial shading conditions, *Energy* 86 (2015) 42–50, <http://dx.doi.org/10.1016/j.energy.2015.03.123>.
- [6] W. Chine, A. Mellit, V. Lughi, A. Malek, G. Sulligoi, A. Massi Pavan, A novel fault diagnosis technique for photovoltaic systems based on artificial neural networks, *Renew. Energy* 90 (2016) 501–512, <http://dx.doi.org/10.1016/j.renene.2016.01.036>.
- [7] A. Dolara, F. Grimaccia, S. Leva, M. Mussetta, E. Ogliari, A physical hybrid artificial neural network for short term forecasting of PV plant power output, *Energies* 8 (2015) 1138–1153, <http://dx.doi.org/10.3390/en8021138>.
- [8] Y.M. Saint-Drenan, S. Bofinger, R. Fritz, S. Vogt, G.H. Good, J. Dobschinski, An empirical approach to parameterizing photovoltaic plants for power forecasting and simulation, *Sol. Energy* 120 (2015) 479–493, <http://dx.doi.org/10.1016/j.solener.2015.07.024>.
- [9] A.K. Tossa, Y.M. Soro, Y. Azoumah, D. Yamegueu, A new approach to estimate the performance and energy productivity of photovoltaic modules in real operating conditions, *Sol. Energy* 110 (2014) 543–560, <http://dx.doi.org/10.1016/j.solener.2014.09.043>.
- [10] A. Dolara, S. Leva, G. Manzolini, Comparison of different physical models for PV power output prediction, *Sol. Energy* 119 (2015) 83–99.
- [11] M. Hejri, H. Mokhtari, M.R. Azizian, M. Ghandhari, L. Söder, On the parameter extraction of a five-parameter double-diode model of photovoltaic cells and modules, *IEEE J. Photovolt.* 4 (2014) 915–923, <http://dx.doi.org/10.1109/JPHOTOV.2014.2307161>.
- [12] S. Kichou, S. Silvestre, G. Nofuentes, M. Torres-Ramírez, A. Chouder, D. Guasch, Characterization of degradation and evaluation of model parameters of amorphous silicon photovoltaic modules under outdoor long term exposure, *Energy* 96 (2016) 231–241, <http://dx.doi.org/10.1016/j.energy.2015.12.054>.
- [13] A.M. Ameen, J. Pasupuleti, T. Khatib, Modeling of photovoltaic array output current based on actual performance using artificial neural networks, *J. Renew. Sustain. Energy* 7 (5) (2015) 1–11, 053107.
- [14] M.F. AlHajri, K.M. El-Naggar, M.R. AlRashidi, A.K. Al-Othman, Optimal extraction of solar cell parameters using pattern search, *Renew. Energy* 44 (2012) 238–245.
- [15] D.H. Muhsen, A.B. Ghazali, T. Khatib, I.A. Abed, A comparative study of evolutionary algorithms and adapting control parameters for estimating the parameters of a single-diode photovoltaic module's model, *Renew. Energy* 96 (2016) 377–389.
- [16] R. Eberhart, J. Kennedy, A new optimizer using particle swarm theory, *MHS'95, Proc. Sixth Int. Symp. Micro Mach. Hum. Sci.* (1995) 39–43, <http://dx.doi.org/10.1109/MHS.1995.494215>.
- [17] M.S. Ismail, M. Moghavvemi, T.M.I. Mahlia, Characterization of PV panel and global optimization of its model parameters using genetic algorithm, *Energy Convers. Manag.* 73 (2013) 10–25, <http://dx.doi.org/10.1016/j.enconman.2013.03.033>.
- [18] J. Ma, Z. Bi, T.O. Ting, S. Hao, W. Hao, Comparative performance on photovoltaic model parameter identification via bio-inspired algorithms, *Sol. Energy* 132 (2016) 606–616, <http://dx.doi.org/10.1016/j.solener.2016.03.033>.
- [19] E. Garoudja, K. Kara, A. Chouder, S. Silvestre, Parameters extraction of photovoltaic module for long-term prediction using artificial bee colony optimization, in: *3rd Int. Conf. Control. Eng. Inf. Technol.*, 2015, pp. 1–6, <http://dx.doi.org/10.1109/CEIT.2015.7232993>.
- [20] V. Jack, Z. Salam, An improved method to estimate the parameters of the single diode model of photovoltaic module using differential evolution, in: *Electric Power and Energy Conversion Systems (EPECS), 4th International Conference, IEEE*, 2015, pp. 1–6.
- [21] M. de Blas, J. Torres, E. Prieto, A. Garcia, Selecting a suitable model for characterizing photovoltaic devices, *Renew. Energy* 25 (2002) 371–380, [http://dx.doi.org/10.1016/S0960-1481\(01\)00056-8](http://dx.doi.org/10.1016/S0960-1481(01)00056-8).
- [22] G. Ciulla, V. Lo Brano, V. Di Dio, G. Cipriani, A comparison of different one-diode models for the representation of I-V characteristic of a PV cell, *Renew. Sustain. Energy Rev.* 32 (2014) 684–696, <http://dx.doi.org/10.1016/j.rser.2014.01.027>.
- [23] L. Hontoria, J. Aguilera, F. Almonacid, G. Nofuentes, P. Zufria, Artificial neural networks applied in PV systems and solar radiation, *Artif. Intell. Energy Renew. Energy Syst.* (2006) 163–200.
- [24] S. Lineykin, M. Averbukh, A. Kuperman, An improved approach to extract the single-diode equivalent circuit parameters of a photovoltaic cell/panel, *Renew. Sustain. Energy Rev.* 30 (2014) 282–289, <http://dx.doi.org/10.1016/j.rser.2013.10.015>.
- [25] T. Ma, H. Yang, L. Lu, Development of a model to simulate the performance characteristics of crystalline silicon photovoltaic modules/strings/arrays, *Sol. Energy* 100 (2014) 31–41, <http://dx.doi.org/10.1016/j.solener.2013.12.003>.
- [26] R. Overstraeten, R. Mertens, Characterisation and Testing of Solar Cells and Modules, Hilger, Bristol, Engl, 1986.
- [27] L. Castañer, S. Silvestre, Modelling Photovoltaic Systems Using PCSpice, 2002, <http://dx.doi.org/10.1002/0470855541>.
- [28] D.L. King, J.a Kratochvil, W.E. Boyson, Photovoltaic array performance model, *Online* 8 (2004) 1–19, <http://dx.doi.org/10.2172/919131>.
- [29] W. De Soto, S.A. Klein, W.A. Beckman, Improvement and validation of a model for photovoltaic array performance, *Sol. Energy* 80 (2006) 78–88, <http://dx.doi.org/10.1016/j.solener.2005.06.010>.
- [30] A.N. Celik, N. Acikgoz, Modelling and experimental verification of the operating current of mono-crystalline photovoltaic modules using four- and five-parameter models, *Appl. Energy* 84 (2007) 1–15, <http://dx.doi.org/10.1016/j.apenergy.2006.04.007>.
- [31] A. Chouder, S. Silvestre, N. Sadaoui, L. Rahmani, Modeling and simulation of a grid connected PV system based on the evaluation of main PV module parameters, *Simul. Model. Pract. Theory* 20 (2012) 46–58, <http://dx.doi.org/10.1016/j.simpat.2011.08.011>.
- [32] J. Peng, L. Lu, H. Yang, T. Ma, Validation of the Sandia model with indoor and outdoor measurements for semi-transparent amorphous silicon PV modules, *Renew. Energy* 80 (2015) 316–323, <http://dx.doi.org/10.1016/j.renene.2015.02.017>.
- [33] C. Sah, R.N. Noyce, W. Shockley, Carrier generation and recombination in P–N junctions and P–N junction characteristics, *Proc IRE* 45 (1957) 1228–1243.
- [34] D. Oliva, E. Cuevas, G. Pajares, Parameter identification of solar cells using artificial bee colony optimization, *Energy* 72 (2014) 93–102, <http://dx.doi.org/10.1016/j.energy.2014.05.011>.
- [35] J.D. Bastidas-Rodríguez, G. Petrone, C.A. Ramos-Paja, G. Spagnuolo, A genetic algorithm for identifying the single diode model parameters of a photovoltaic panel, *Math. Comput. Simul.* (2015), <http://dx.doi.org/10.1016/j.matcom.2015.10.008>.
- [36] R. Storn, K. Price, Differential evolution – a simple and efficient heuristic for global optimization over continuous spaces, *J. Glob. Optim.* 11 (1997) 341–359, <http://dx.doi.org/10.1023/A:1008202821328>.
- [37] D. Karaboga, B. Akay, A comparative study of Artificial Bee Colony algorithm, *Appl. Math. Comput.* 214 (2009) 108–132, <http://dx.doi.org/10.1016/j.amc.2009.03.090>.
- [38] I.A. Ibrahim, A. Mohamed, T. Khatib, Modeling of photovoltaic array using random forests technique, in: *Conference on Energy Conversion (CENCON), IEEE*, 2015, October, pp. 390–393.